RESEARCH ARTICLE

Key Points:
- Storm-induced plasma density irregularities/scintillations over Indian longitude
- Impact of prompt penetration electric fields on PRE, *h'F*, and EIA density
- Suppression of EIA on the following day due to disturbance dynamo

Correspondence to:
S. Sripathi,
ssripathi.iig@gmail.com

Low-latitude ionosphere response to super geomagnetic storm of 17/18 March 2015: Results from a chain of ground-based observations over Indian sector

Ramsingh[1], S. Sripathi[1], Sreeba Sreekumar[1], S. Banola[1], K. Emperumal[2], P. Tiwari[3], and Burudu Suneel Kumar[4]

[1]Indian Institute of Geomagnetism, Navi Mumbai, India, [2]Equatorial Geophysical Research Laboratory, Indian Institute of Geomagnetism, Tirunelveli, India, [3]KSK Geophysical Research Laboratory, Allahabad, India, [4]TIFR Balloon Facility, Hyderabad, India

Abstract In this paper, we present unique results of equatorial and low-latitude ionosphere response to one of the major geomagnetic storms of the current solar cycle that occurred during 17–18 March 2015, where *Dst* reached its minimum of −228 nT. Here we utilized data from magnetometers, chain of ionosondes located at Tirunelveli (8.73°N, 77.70°E; geometry: 0.32°N), Hyderabad (17.36°N, 78.47°E; geometry 8.76°N), and Allahabad (25.45°N, 81.85°E; geometry 16.5°N) along with multistation GPS receivers over Indian sector. The observations showed a remarkable increase of *h'F* to as high as ~560 km over Tirunelveli (magnetic equator) with vertical drift of ~70 m/s at 13:30 UT due to direct penetration of storm time eastward electric fields which exactly coincided with the local time of pre-reversal enhancement (PRE) and caused intense equatorial spread *F* irregularities in ionosondes and scintillations in GPS receivers at wide latitudes. Plasma irregularities are so intense that their signatures are seen in Allahabad/Lucknow. Storm time thermospheric meridional winds as estimated using two ionosondes suggest the equatorward surge of gravity waves with period of ~2 h. Suppression of anomaly crest on the subsequent day of the storm suggests the complex role of disturbance dynamo electric fields and disturbance wind effects. Our results also show an interesting feature of traveling ionospheric disturbances possibly associated with disturbance meridional wind surge during recovery phase. In addition, noteworthy observations are nighttime westward zonal drifts and PRE-related total electron content enhancements at anomaly crests during main phase and counter electrojet signatures during recovery phase.

1. Introduction

The electrodynamics of the equatorial and low-latitude ionosphere are significantly modified during major geomagnetic storms due to electrical, neutral, and electrodynamical coupling of the high-latitude processes such as magnetospheric convection and particle precipitation. Since storm time is characterized by the increased energy as well as momentum deposition over high latitudes due to the particle precipitation, Joule heating, and the convection electric fields, these enhancements, subsequently, can couple to equatorial and low-latitude ionosphere and may cause significant changes in the plasma density redistribution and drift motions in those regions. There are two types of electric fields that can penetrate to the equatorial and low-latitude ionosphere and can influence low-latitude electrodynamics. They are (a) prompt penetration (PP) electric fields which are of short duration (~1–2 h) and (b) long-lasting disturbance dynamo (DD) electric fields (>3 h) [*Kikuchi*, 1986; *Araki et al.*, 1985; *Blanc and Richmond*, 1980]. While the prompt penetration electric fields occur whenever large or rapid changes in the magnetospheric convection electric fields, disturbance dynamo electric fields are caused due to particle precipitation resulting in the heating of the high-latitude thermosphere leading to the changes in thermospheric circulation pattern. The PP electric fields can be understood in terms of relative strengths of region 1 and region 2 field-aligned currents. It may be mentioned that a sudden southward turning of the *z* component of the interplanetary magnetic field (i.e., IMF B_z), from a steady northward configuration, produces a dawn to dusk convection electric field at high latitudes resulting in an undershielding condition [*Somayajulu et al.*, 1987; *Huang et al.*, 2005; *Kikuchi et al.*, 2008]. This electric field will be eastward during daytime and westward during nighttime. This undershielding electric field being active in the main phase of the storm will map directly to the equatorial and low latitudes from the magnetosphere through the propagation of hydromagnetic wave [*Kikuchi*, 1986; *Araki et al.*, 1985].

However, this steady southward IMF B_z configuration may not exist for long and the IMF B_z will turn northward again, and subsequently, overshielding condition prevails. This overshielding electric field becomes active in the recovery phase. Thus, the existing region 2 electric field penetrates to the equatorial and low latitudes [*Kelly et al.*, 1979; *Kikuchi et al.*, 1996]. Recent study by *Huang* [2008] showed that PP electric fields can map to low latitudes for significantly longer durations of ~8–10 h, if IMF B_z is southward for prolonged period.

Contrary to PP electric fields, the time required to build up the DD electric fields is too large (greater than 3 h). Since these electric field disturbances are long-lasting and vary more slowly, the response of low-latitude ionosphere can be seen up to about a day or two after the onset of geomagnetic storm [*Blanc and Richmond*, 1980; *Sastri*, 1988; *Fejer et al.*, 1983]. Apart from this, enhanced storm time Joule heating in the auroral zone results in the generation of atmospheric gravity waves (AGWs) or traveling atmospheric (ionospheric) disturbances [*Richmond and Matsushita*, 1975; *Lee et al.*, 2002; *Lei et al.*, 2008] that can transport ionized particles to low latitudes with an increase in temperature and N_2 density resulting in a decrease in the [O]/[N_2] ratio and decrease in ionization [*Mikhailov and Schlegel*, 1998] and an increase in the recombination coefficient caused by high temperatures [*Buonsanto*, 1999]. This large-scale AGW's interaction with the neutral circulation during storm time can lead to the equatorward/poleward neutral wind surge. Because of these rapid fluctuations in the direction and amplitude of meridional neutral winds, it can serve as an important factor in plasma transport and hence significantly affect the densities in the low latitudes.

Several authors have described dramatic ionospheric effects at low latitudes related to strong magnetic storms, observed by various techniques such as ionosondes, optical airglow measurements, or satellite probes [e.g., *Abdu et al.*, 2003; *Basu et al.*, 2001; *Batista et al.*, 1991; *Sastri et al.*, 2002]. Many interesting results have also been reported by Indian scientists from Indian sector [e.g., *Rastogi*, 1974; *Somayajulu et al.*, 1987; *Sastri et al.*, 2000]. Often, ionospheric plasma distribution is affected by the storm time ionospheric electric field perturbations, by creating positive ionospheric storm (increase in f_oF_2) and/or negative ionospheric storm (decrease in f_oF_2). In a recent study using multiinstrument and multistation data over Indian longitude, *Bagiya et al.* [2011] observed that the significant variations to the ionospheric parameters and phenomena like equatorial ionization anomaly (EIA) and equatorial electrojet (EEJ) in terms of positive and negative ionospheric storms occurred during 15–17 May 2005, respectively. Chemical effects of the storm time equatorward neutral winds could cause negative ionospheric storms, which increase the N_2 concentration in thermosphere and decrease the O concentration [e.g., *Fuller-Rowell et al.*, 1994]. However, positive ionospheric storms are produced by additional production of density at lower altitudes due to photoionization as existing density goes to higher altitudes due to higher upward drifts [*Lin et al.*, 2005; *Sastri et al.*, 2000]. They also suggested that equatorward winds and waves also produce positive storms.

The increase in solar wind and high plasma density near heliospheric current sheet during storm time can cause increase in ram pressure into the magnetosphere. Hence, near the geomagnetic equator, the response of EEJ currents to this interaction can vary and can be detected by ground-based magnetometers [*Tsurutani et al.*, 2006]. Sometimes, EEJ currents also reverse its direction to westward (known as counter electrojet (CEJ)) during geomagnetic storms as a depression in diurnal variations of H component geomagnetic field measured over the equatorial regions [*Rastogi*, 1974; *Somayajulu et al.*, 1993]. In addition, during geomagnetic storms, an additional ionization layer called F_3 layer also can be seen as a result of upward plasma drift and meridional neutral winds. It is believed that strong magnetic storms associated with changes in the IMF B_z could result in the decrease of F_2 layer critical frequency (f_oF_2) over the magnetic equator and leads to the formation of an additional layer (F_3) above the F_2 peak [*Balan et al.*, 2008]. *Sreeja et al.* [2009] studied the effect of storm over the equatorial and low-latitude ionosphere on the basis of development/inhibition of EIA and the generation/inhibition of equatorial spread F (ESF) as well as on the development of F_3 layer. Under the action of disturbance electric fields, equatorial plasma fountain can be significantly enhanced/suppressed, which in turn is responsible for the variations in the EIA. During daytime, storm-induced PP electric fields due to the undershielding condition are eastward, which will add up to the preexisting electric field and can lead to an enhancement in the upward vertical $E \times B$ drift at the equator. Sometimes, this PP electric field can be so large (~3–4 mV/m) that they can produce the superplasma fountain effect at the equator [*Tsurutani et al.*, 2004]. This is responsible for the poleward expansion of the ionization anomaly along with enhancement in the low-latitude ionization density. However, it is argued that major enhancement comes from local production of ionization due to photoionization at low latitudes than

transport of ionization from a remote location as suggested by *Rishbeth et al.* [2010]. Geomagnetic storms can significantly disturb the global ionosphere and upper atmosphere, giving rise to noticeable variations in ionospheric parameters like total electron content (TEC), F_2 layer peak density (N_mF_2), and its height (h_mF_2). Reduction in TEC during the daytime can occur as a consequence of DD electric field of westward polarity and hence results in the contraction of the EIA [*Tsurutani et al.*, 2004], whereas eastward polarity of the DD electric field during nighttime can lead to increase in the F layer uplift, which in turn results in the intensification of EIA [*Abdu*, 1997].

In the present study, we examine the ionosphere response to one of the major storms of the current solar cycle (solar cycle 24), which occurred on 17 March 2015, following double-halo coronal mass ejections (CMEs) that hit the Earth's magnetosphere at ~04:30 UT. Two large eruptions that left the Sun on 15 March 2015 caused this G4 storm. These two Earth-directed CMEs added and accelerated together through interplanetary space, resulting in the large geomagnetic storm with DST index decreasing to its minimum of −228 nT. Since *Dst* reached −228 nT during this storm period which is the largest of the current solar cycle so far, we consider this storm as a superstorm here. Although it initiated as a low-intensity storm (G1 class), later it got intensified into a G4 class storm, making it the strongest storm of the current solar cycle. According to NOAA (http://www.swpc.noaa.gov/NOAAscales/), G4 storm is considered as a "severe" storm when *Kp* reaches 8 including 9−. The ΣKp of 48 and *Ap* index of 108 for this storm suggest that it is an intense geomagnetic storm. Since each storm is unique in the sense that it is characterized by strength, shock impact orientation, and duration of southward IMF B_z, geoeffectiveness of these storms in terms of ionospheric response is also distinctive. Hence, the aim of this paper is to understand the response of equatorial and low-latitude ionospheric processes such as ESF, EIA, and EEJ strength to such major storm and compare these variations with geomagnetically quiet day using chain of ionosondes and GPS receivers over India.

2. Data Sets Used in the Present Analysis

We analyzed multiinstrument data over equatorial and low-latitude ionosphere to study their response to the intense geomagnetic storm of 17 March 2015. The geomagnetic activity indices like *Kp*, *AE*, and *SYM-H* (high-resolution ring current) are obtained from World Data Center (WDC), while ionospheric parameters, namely, $h'F$, h_pF_2, and f_oF_2, are scaled for the period of 16 to 18 March by using data obtained from three Canadian Advanced Digital Ionosondes (CADIs) operating at an equatorial station, Tirunelveli (8.73°N, 77.70°E); low-latitude station, Hyderabad (17.36°N, 78.47°E; geometry 8.76°N); and a northen edge of the crest region, Allahabad (25.3°N, 81.5°E), respectively. While ionogram at Tirunelveli is collected at 10 min interval initially, later on, it is operated at 5 min interval after identifying the progress of the ongoing space weather event. However, CADI at Hyderabad was operated at every 15 min interval. Similarly, although we collected ionograms at Allahabad at every 15 min interval initially, later on, we operated it at 5 min interval. However, the Doppler drift mode of observations at 1–8 MHz frequencies at Tirunelveli/Hyderabad/Allahabad is operated at 1 min interval continuously.

Simultaneously, we collected TEC and L band scintillations from the GPS receiver (SCIntillation Network Decision Aid (SCINDA)) at Tirunelveli/Rajkot and Global Navigation Satellite Systems (GNSS) receiver at Nagpur. We also utilized TEC obtained from International GPS Service (IGS) station at Bangalore/Hyderabad/Lucknow for the same period under investigation so as to provide wide spatial coverage over Indian region. Here it may be mentioned that due to the dispersive nature of the ionosphere, the radio signals used in GPS/GNSS receivers that propagate at different phase velocities produce a time delay. This time delay is proportional to the electron density along the line of sight between the receiver and the satellite. From this, slant TEC (STEC) is obtained. The vertical TEC (VTEC) is obtained using appropriate mapping function, $S_f = \cos \chi$; i.e., VTEC = STEC* $\cos \chi$, where $\chi = \sin^{-1}[R_E \cos \alpha/(R_E + h)]$, α is the elevation angle at ionospheric penetration point, $R_E = 6378$ km, and $h = 350$ km. The horizontal components of Earth's magnetic field (1 min resolution) measured by the ground-based magnetometers at Tirunelveli (H_{TIR}) (8.73°N, 77.70°E), an equatorial station and Alibag (H_{ABG}) (18.5°N, 72.9°E), an off-equatorial station (located outside the EEJ influence) in Indian longitude are used for estimating EEJ strength which is the difference of ΔH_{TIR} and ΔH_{ABG}. Longitudinal variations have been studied using data from South American and South African sectors by using the ionosonde and GPS TEC. Figures 1a and 1b show the locations of various stations used in the present study along with their field line mapping. For details, see Table 1 which shows the list of stations along with instruments as used in the present study.
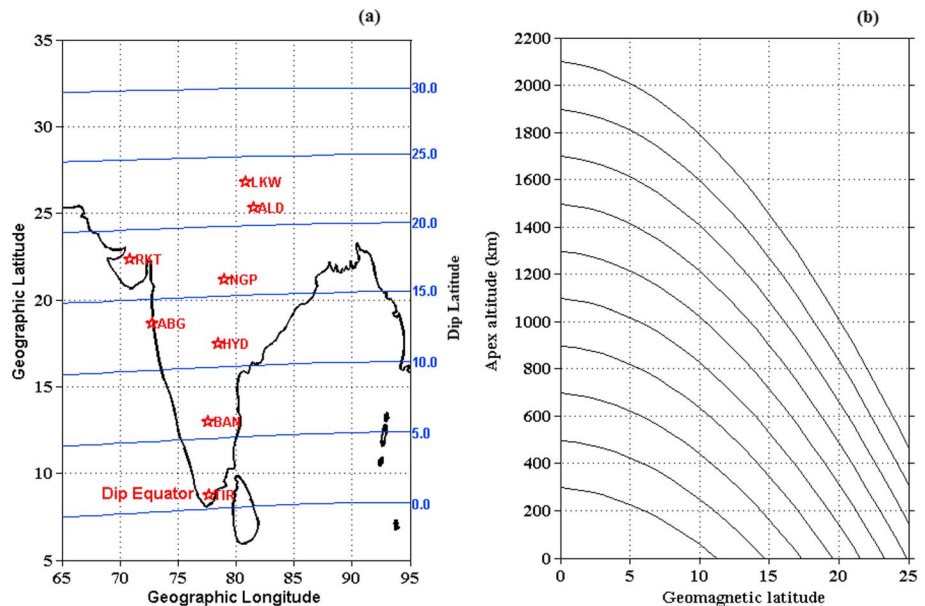
Figure 1. (a) The location of stations used in the present analysis and (b) the latitude-altitude variation of field line geometry.

3. Results

3.1. Interplanetary and Geomagnetic Conditions During 17–18 March 2015

Figures 2a–2h show the 1 min variations in the solar wind parameters (in GSM coordinates) from the ACE satellite at L_1 point, namely, solar wind pressure; solar wind speed; interplanetary magnetic field (IMF) B_z; and interplanetary electric field (IEFy) along with geomagnetic activity indices like AE (AU/AL) index, SYM-H index, EEJ strength, and Kp index, respectively, for the period of 16 to 18 March 2015. During this storm period, variation of average solar wind speed of ~550–600 km/s, solar wind pressure of 20–30 nPa, interplanetary magnetic field of −25 to 20 nT, and IEFy electric fields of ±10 mV/m are noticed. Here it may be noted that the convection time delay of 47 min from ACE to magnetosphere was estimated and is corrected while plotting the solar parameters in order to match with other ground-based observations. From the figure, it can be seen that on 16 March, the day prior to the storm onset, Kp, AE (AU/AL), and SYM-H indices are varied as per quiet time variations. However, later on, the figure gives a clear picture of the intense geomagnetic storm, following a double-halo CME that hits the Earth's magnetic field approximately 04:45 UT on 17 March 17 2015. Initially, the IMF B_z went northward turning for a while, indicating storm sudden commencement (SSC) before it suddenly turned southward at nearly 06:00 UT. After reaching to −25 nT, the IMF B_z went back to northward at ~07:00 UT for a brief time with magnitude of 20 nT, and again, it was oscillating between north/south turning at a faster rate before it turned southward at 08:00 UT. After that, IMF B_z slowly went back to northward at 12:00 UT before it again turned southward. However, after that, the IMF B_z continued for a long time, i.e., 12 h in the southward direction with a magnitude of −20 nT. It again turned northward after 00:00 UT on 18 March 2015.

Table 1. List of Stations Used in Our Study

| Station	Instrument	Geographic Latitude	Geographic Longitude	Geomagnetic Latitude
Tirunelveli (TIR)	CADI and SCINDA GPS receiver	8.73°N	77.7°E	0.23°N
Bangalore (BAN)	IGS GPS station	12.97°N	77.59°E	4.44°N
Hyderabad (HYD)	CADI and IGS GPS station	17.36°N	78.47°E	8.76°N
Nagpur (NGP)	GNSS receiver	21.14°N	79.08°E	12.42°N
Rajkot (RKT)	SCINDA GPS receiver	22.30°N	70.93°E	14.21°N
Allahabad (ALD)	CADI	25.43°N	81.84°E	16.48°N
Lucknow (LKW)	IGS GPS station	26.85°N	80.92°E	17.69°N
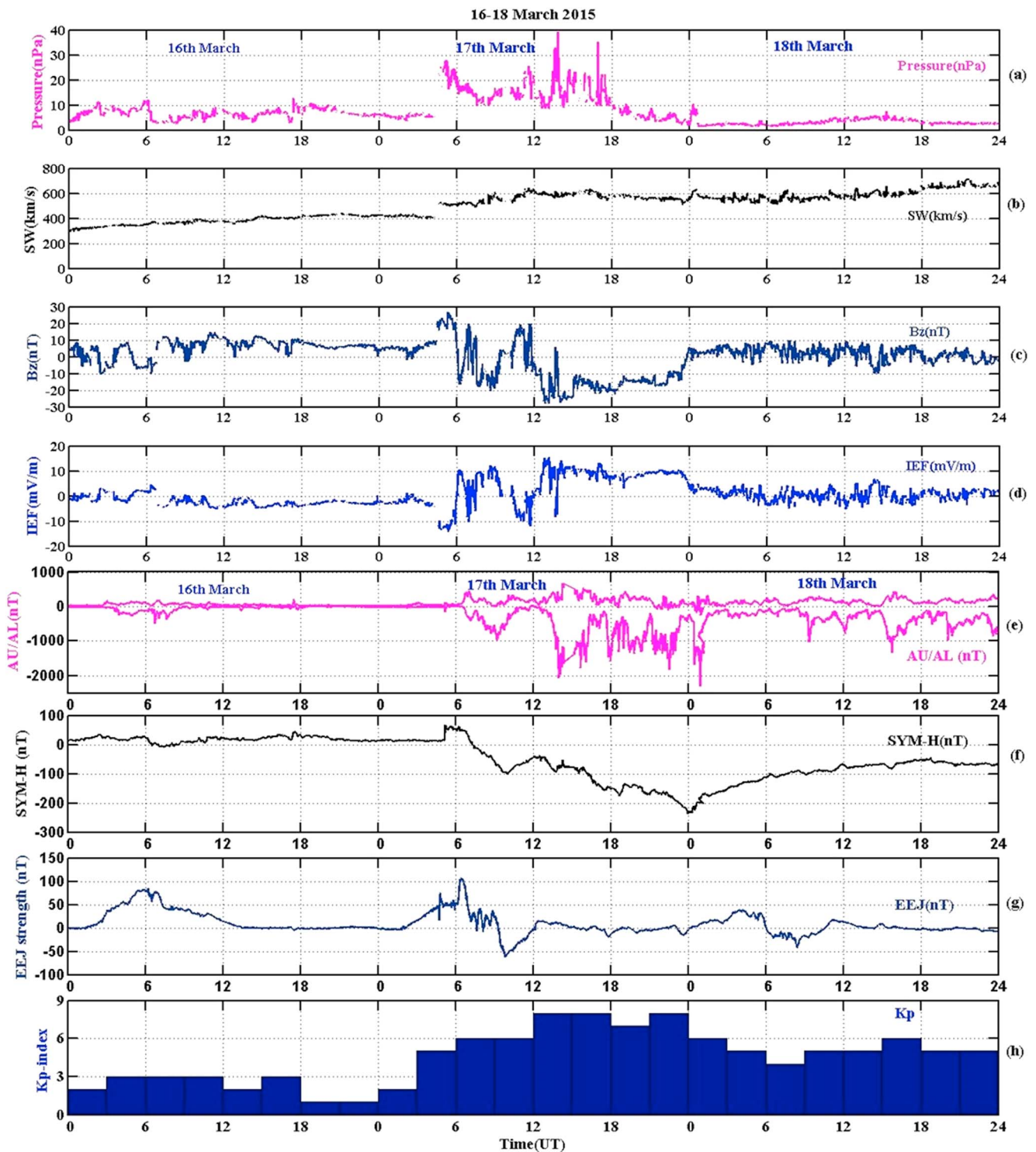
Figure 2. Temporal variations in (a) solar wind pressure, (b) speed, (c) IMF B_z, and (d) IEF in GSM coordinates for the period of 16 to 18 March 2015 and geomagnetic indices, namely, (e) AE (AU/AL) index, (f) SYM-H, (g) EEJ strength, and (h) Kp index for the same period are shown.

So the IMF B_z was almost southward for about ~18 h with a brief northward turnings in between. Similarly, IEFy was varying between dawn and dusk as per the IMF B_z variations.

Meanwhile, the Kp values which were initially in the range of 5 increased up to 8 and $SYM\text{-}H$ index, which is high-resolution Dst index, reached a maximum of up to -228 nT at 00:00 UT on 18 March 2015. This was followed by the onset of multiple substorms which is clearly visible from AE (AU/AL) index, which is an indicator of auroral electrojet activity, immediately after the main phase of the storm onset as can be seen in the figure. Meanwhile, in $SYM\text{-}H$, SSC started immediately followed by IMF B_z northward turning prior to southward turning that increased magnetic flux density at the magnetopause region. It is seen that after 06:00 UT, the main phase of the storm started, followed by a decrease in the H component of the geomagnetic field implying intensification of westward ring current. In the recovery phase which is characterized by an increase in the H component shows slow recovery to normal behavior on 18 March.

On the other hand, EEJ showed normal quiet time variations on 16 March. However, on 17 March, initially, the EEJ strength variations are normal up to 06:00 UT. However, a strong EEJ of ~100 nT is observed during 06:20 UT as a consequence of a sudden turning of IMF B_z to southward due to undershielding effect, where prompt penetration of eastward electric fields map to low latitudes during daytime. After that, EEJ had undergone multiple fluctuations showing similar variations as of IMF B_z until 08:00 UT. Immediately, EEJ reversed to CEJ where its strength reached to -50 nT at 10:00 UT. This exactly coincides with northward turning of IMF B_z which could have produced westward electric fields due to overshielding effect. However, after that, it again gradually returned back to normal behavior. On 18 March 2015, the EEJ strength was ~50 nT at 04:00 UT (in the morning) but noontime CEJ is observed from 06:00 to 11:00 UT. This day is mostly influenced by the disturbance dynamo electric fields under which westward electric fields are imposed on the existing eastward electric fields. Due to increased westward electric fields, it overcomes local eastward electric fields and can cause depression in delta H.

3.2. Storm Time Ionospheric Response as Seen by Chain of Ionosondes

In order to study the influence of this storm on equatorial and low-latitude ionosphere, we analyzed the ionosonde data in terms of virtual height, h_pF_2 (peak height), and f_oF_2 (N_mF_2) at Tirunelveli/Hyderabad/Allahabad stations during 16–18 March 2015 which are shown in Figures 3a–3g. While 16 March is considered here as quiet day as Ap index is just 12, other 2 days are considered as storm days. Figures 3a–3c show the f_oF_2 (MHz) variations over Tirunelveli, Hyderabad, and Allahabad, respectively; Figures 3d–3f show the ionospheric parameters, namely, h_pF_2 (peak height) in black color and $h'F$ (virtual height) in green color over Tirunelveli, Hyderabad, and Allahabad, respectively. Figure 3g shows the IMF B_z during 16–18 March 2015. The black line in f_oF_2 plots show the duration of ESF at that station. It may be noted that data gaps in f_oF_2 (MHz), $h'F$ (km), and h_pF_2 (km) over Hyderabad/Allahabad stations are due to blank/bad ionogram traces. The temporal variations of f_oF_2, $h'F$, and h_pF_2 on 16 March show normal behavior and behave as per EEJ variations. During nighttime reduction of density at all the stations due to absence of production and daytime increase of density at all the stations due to photoionization are noticed. Allahabad station has seen enhanced density on 16 March due to strong fountain effect. However, on the storm day, i.e., 17 March, f_oF_2 behaved normally up to 04:30 UT. But immediately after that, density variations are found to behave as per IMF B_z variations at all the stations. The two patches of F_3 layer started occurring on 17 March during SSC period and at the time of southward turning which was absent on other 2 days as can be seen in the figure. This also coincides with EEJ fluctuations as shown in Figure 2, indicating that this could be the result of strong fluctuations in zonal electric field on 17 March as compared to other 2 days. Strong reduction of density over Tirunelveli increases the density at low latitudes due to fountain effect under the influence of eastward PP electric fields over Tirunelveli due to undershielding effect. However, northward turning of IMF B_z at 09:30 UT caused westward EEJ currents and westward electric fields which increased the density over Tirunelveli and h_pF_2 reduced drastically. This reduction of h_pF_2 is seen at all the stations at this time. Immediately after that, IMF B_z turned southward at 12:00 UT, and again, it went abruptly for a short duration at 13:30 UT which might have triggered eastward PP electric field to equator and virtual height went to very high altitude, i.e., 560 km. Same time, there was also increase of virtual height at Hyderabad/Allahabad stations, indicating that they are electric field driven. Almost same time, density (f_oF_2) over Tirunelveli got reduced drastically and this increased the density at low latitudes (see TEC plots). But due to blank ionogram traces at Hyderabad/Allahabad, we are
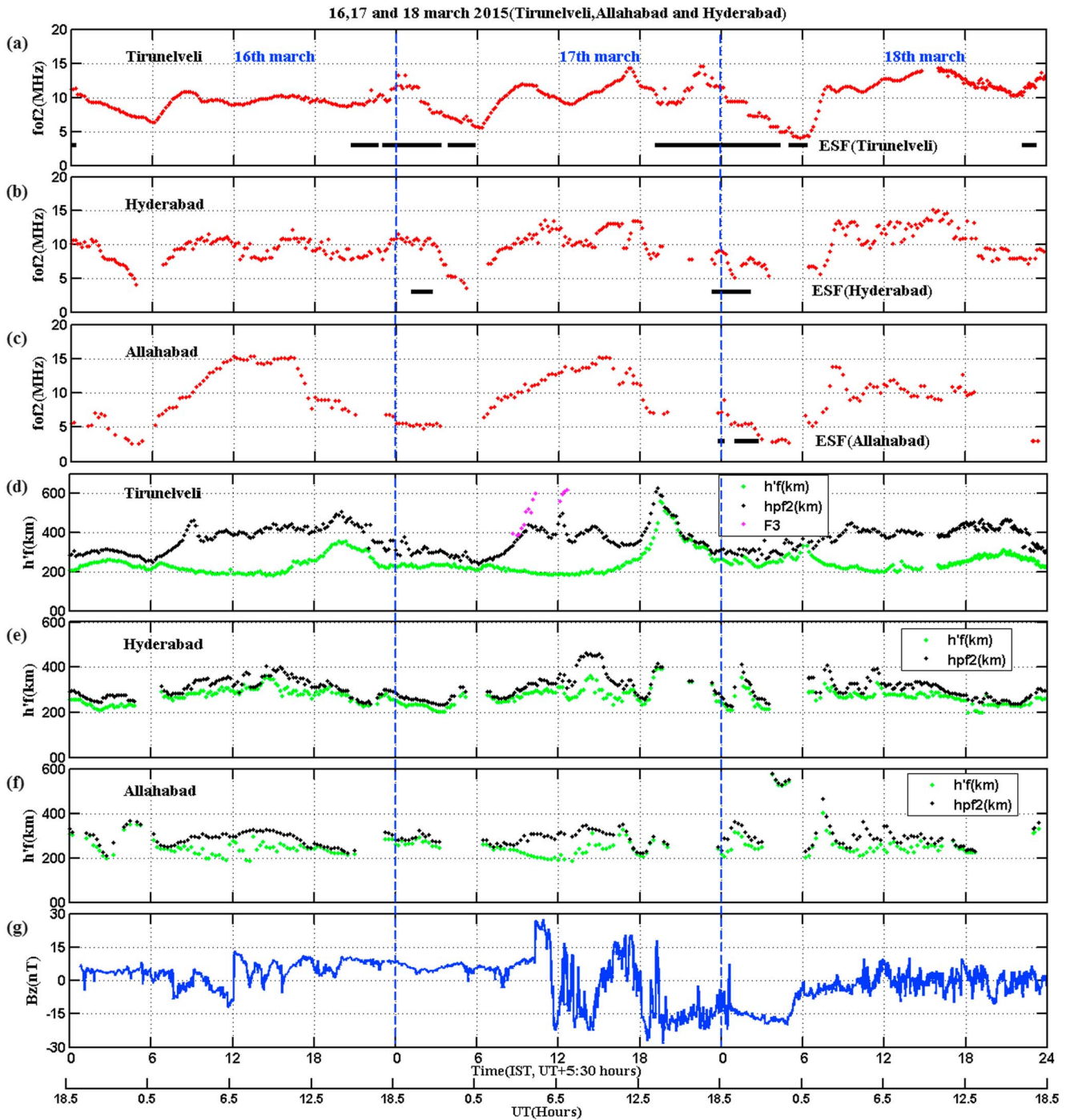
Figure 3. The temporal variations of ionospheric F region density in terms of f_oF_2 in MHz (red) for (a) Tirunelveli, (b) Hyderabad, and (c) Allahabad. $h'F$ in km (green) and h_pF_2 in km (peak height) (black) for (d) Tirunelveli, (e) Hyderabad, and (f) Allahabad, respectively, during 16–18 March 2015. F_3 layer (magenta) is also visible in Figure 3d. (g) These figures are supported by B_z for comparison.

unable to see crest enhancements properly. The enhancements in both $h'F$ and h_pF_2 at 12:30 UT on 17 March could be attributed to the southward turning of IMF B_z in conjunction with the prompt penetration (PP) eastward electric field, where this eastward PP electric field will add up to the ambient zonal electric field (due to the F region dynamo) giving rise to the enhanced upward $E \times B$ drift. This enhanced F region height rise led to the intense ESF in ionosonde on 17 March for more than 10 h starting from 13:50 UT (19:20 India standard time (IST)) to next day 00:50 UT (06:20 IST). The spread F was so intense that we could see spread F signatures

in Allahabad in the postmidnight of 17 March which we notice rarely. However, although ESF was observed at Tirunelveli on the previous night with lesser intensity, $h'F$ did not go to very high altitude unlike 17 March. In fact, we have examined all days during March 2015 to conclude that none of the day's height in the evening is raised to very high altitude except on 17 March. So we consider this as significant height rise and it could be caused due to PP electric fields. During this period, AE (AU/AL) index showed reducing its AL value to a value of ~ -2000 nT. This AL reduction suggests strong prompt penetration of the auroral electric field to low latitudes due to storm time substorm. There is a reduction of $ASY\text{-}H$ index (not shown here) at the same time, indicating the particle injection into ring current leading to the partial ring current intensification. Immediately, strong equatorial spread F (ESF) started occurring at Tirunelveli as indicated by the black line. Large pre-reversal enhancement (PRE) in zonal electric fields could have favored the ESF generation. Following this, f_oF_2 (density) started decreasing at Tirunelveli. However, electron density started again increasing at 15:00 UT, and it reached a maximum of 15 MHz before density again started decreasing slowly and height also started decreasing. The density reached its minimum of 4.5 MHz at 00:30 UT on 18 March 2015. Again, electron density started increasing drastically and reached 12 MHz at 08:30 UT on 18 March 2015. After that, the density shows oscillatory behavior with three to four bumps. The h_pF_2 over Tirunelveli also shows such oscillatory behavior at this time on this day. The density, h_pF_2, and $h'F$ over Hyderabad and Allahabad stations also show such oscillatory behavior in their temporal variations. However, the mean density over Allahabad is significantly reduced on 18 March 2015 than the other 2 days. The oscillatory features are more clearly visible on 18 March 2015, where the storm is still in the recovery phase. This oscillatory behavior over Hyderabad/Allahabad can be due to the role of meridional neutral winds by the disturbance winds where poleward neutral wind results in decrease of h_pF_2, whereas equatorward winds cause an increase in h_pF_2.

3.2.1. Equatorial Vertical/Zonal Plasma Drifts as Seen in Tirunelveli Ionosonde

Figure 4a shows the vertical Doppler drifts from Doppler drift mode of observations at 7 MHz over Tirunelveli during 16–18 March 2015. Here it may be mentioned that during daytime, Doppler drifts as shown in the figure may not represent correct drifts due to photoionization and lack of sufficient irregularities. However, these drifts can provide meaningful information during nighttime only when irregularities are sufficient in number. So to substantiate, we also show evening time vertical drifts obtained from the rate of change of virtual height ($h'F$ (km)) at 4 MHz during 16–18 March 2015 in Figure 4a in green color. From Figure 4a, it can be seen that only quiet day variations can be seen on 16 March. However, in contrast, on 17 March, vertical drift indicative of strong vertical drift fluctuations during daytime and at the same time F_3 layer started occurring as can be seen in Figure 3d. However, vertical drift goes up to 70 m/s at 13:30 UT (19:00 IST) as can be seen in the figure. The vertical drift obtained from $h'F$ (green) also shows the similar magnitude of drift as that of Doppler drift at almost the same time. Small variations in time as seen in the plot could be due to varying resolutions at which they are obtained. This large value of PRE and associated evening height increase of the F layer at Tirunelveli are sufficient for the generation of equatorial spread F irregularities.

Figures 4b and 4c show the variation of (a) vertical and (b) zonal plasma drifts from a Doppler drift mode of CADI observations over Tirunelveli during 15:30–20:30 UT on 17/18 March 2015 which is quite similar to that of Figure 4a. This figure is shown here to show the late night variation of drifts on 17/18 March 2015. For comparison, 16 March 2015 is also plotted in blue color. The variations in the vertical drifts suggest that they are significantly varied as compared to 16 March. Similarly, zonal drifts show that they also varied drastically as compared to 16 March night. The zonal drift was westward on this night as compared to 16 March. The maximum zonal drifts of -70 m/s were seen at 17:45 UT (23:15 IST), which is just prior to vertical drifts that went down to -30 m/s. Such drifts were presented earlier over Brazilian region by *Abdu et al.* [2003] but seldom reported over Indian sector. These variations suggest that there was strong disturbance dynamo present on this night apart from PP electric fields.

3.2.2. Plasma Irregularities as Seen in Ionosondes

Figures 5a and 5b show the sample ionogram traces of ESF irregularities over Tirunelveli (TIR) and Allahabad (ALD) on 17–18 March 2015 night. While the ionogram traces over TIR show postsunset period, the same is shown for the postmidnight period over ALD. The ionogram shows that F layer height went drastically upward on 17 March at TIR. On postmidnight of 17 March (18 March early morning), both the stations TIR and ALD show spread F. While ESF was present from 19:30 to 06:20 IST on 17 March at Tirunelveli, Allahabad showed signatures of spread F only in the postmidnight on 17 March 2015, i.e., from 00:00 IST to 1:45 IST on 18 March 2015. After that, traces over ALD were not clear. It has been reported by
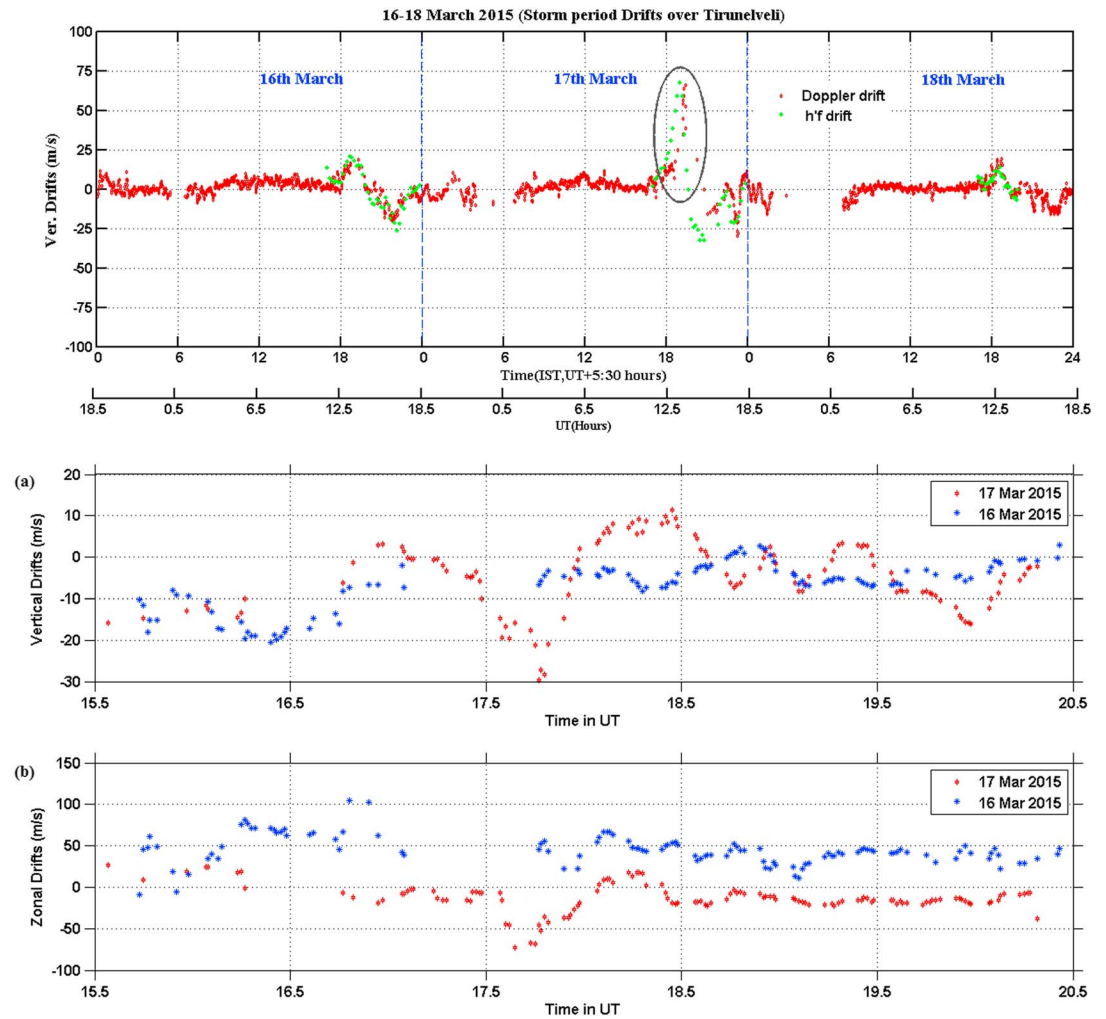
Figure 4. (a) The Doppler vertical drifts over Tirunelveli as obtained from CADI ionosonde during 16–18 March 2015. Also shown is the vertical drift obtained from rate of change of virtual height ($h'F$ (km)) on 16–18 March 2015 (green). Drifts of ~70 m/s due to PPEF on 17 March are highlighted by oval shape. The portion of (b) vertical and (c) zonal drifts at 15.5–20.5 UT on 17 March 2015 (storm time; red) and on 16 March 2015 (quiet time; blue) for one to one comparison.

Huang et al. [2007] that during intense storms, depleted flux tubes associated with large-scale equatorial plasma bubbles might have extended to 40–50° magnetic latitudes. Spread *F* signatures in ALD indeed suggest the role of strong eastward electric fields over Indian longitude. In our study, eastward prompt penetration of electric fields associated with southward IMF B_z occurs around 19:00 IST, and nearly within 30 min, the postsunset spread *F* began. Due to this eastward PPE, the zonal eastward electric field gets enhanced and thereby enhancement occurs in the PRE which leads to the postsunset *F* region height rise, and hence, the layer is taken to higher altitudes where Rayleigh-Taylor (RT) instability growth rates could be favored and leading to spread *F* irregularity generation. In postmidnight, spread *F* continues at TIR. At ALD, PPEF effect is not very significant due to the fact that the efficiency of the electric field penetration reduces at low latitudes as magnetic field lines are inclined. But in ALD, spread *F* started occurring only during midnight. This could be due to the fact that irregularities over Tirunelveli could have to rise to very high altitude so that we could be able to see them over ALD.

3.2.3. Thermospheric (Nighttime) Meridional Winds as Deduced From Ionosondes

In order to investigate thermospheric meridional winds during 17–18 March 2015, we estimated thermospheric meridional neutral winds using two ionosondes, in which one is located at the equator (here Tirunelveli) and other is located away from the equator (here it is Hyderabad) using the method described by *Krishna Murthy et al.* [1990]. Using this method, it is possible to obtain thermospheric
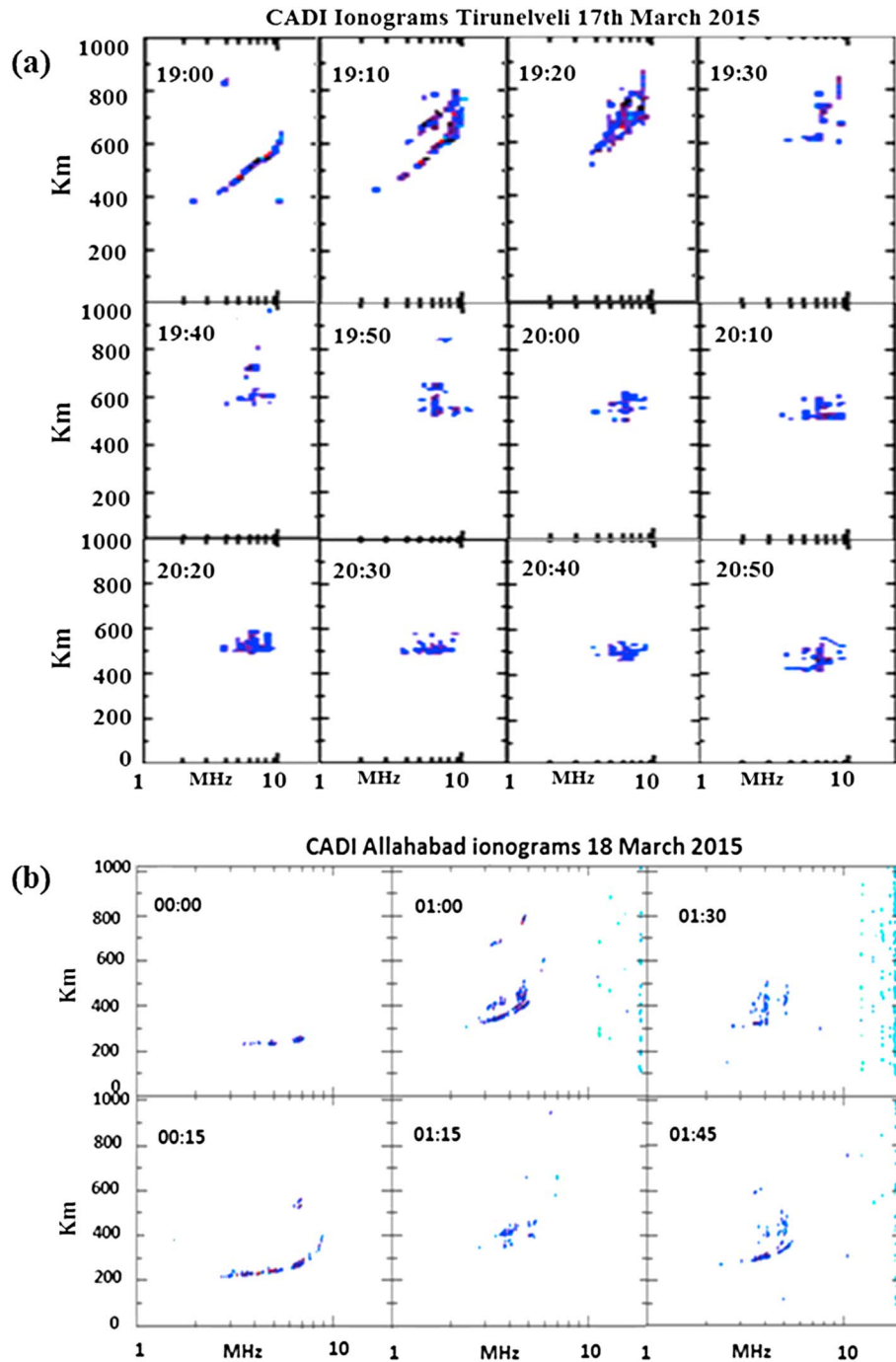
Figure 5. Ionogram images of ESF over (a) Tirunelveli and (b) Allahabad as obtained from CADI on 17–18 March 2015 (night).

meridional winds to a reasonable value after taking care of recombination effects. Figure 6 show the thermospheric meridional winds during 18:00–22:00 UT on 17/18 March 2015 at every 15 min interval as calculated using above method. The figure suggests that there were lot of fluctuations in the magnitude of winds. It appears that these fluctuations are associated with gravity wave activity with period of 2 h. *Sastri et al.* [2000] have studied the thermospheric winds using same method, and they found large-scale fluctuations in the wind resembling gravity waves. Our observations as presented here also show similar features reiterating the fact that thermospheric winds are drastically modified on 17/18 March 2015 night.
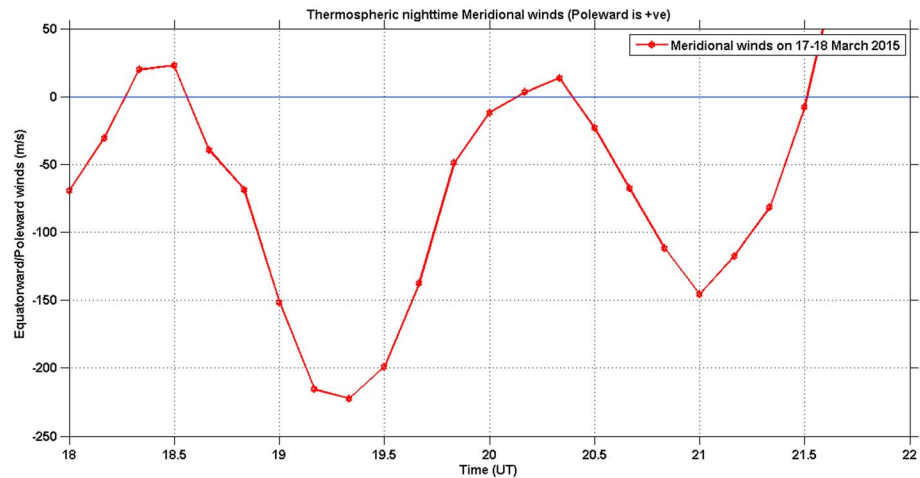
Figure 6. The calculated meridional winds during 18:00–22:00 UT on 17 March. Blue line represents transition from poleward to equatorward winds.

3.2.4. Traveling Ionospheric Disturbances (TIDs) During Recovery Phase

Figures 7a and 7b show the simultaneous observations of temporal variation of CADI isodensity profiles at 5–7 MHz frequencies at Hyderabad and 5–8 MHz frequencies at Allahabad stations during 03:00–10:00 UT on 18 March 2015. The black vertical lines indicate phase propagation. This kind of plots will be useful to understand whether these variations are due to electric field-driven or neutral wind-driven variations. If it is electric field driven, the same variations can be seen at both places. The figure shows that there were large-scale wave like oscillations but there is a phase lag. Keen observations suggest that these oscillations occur first at Allahabad and later at Hyderabad. Based on the phase delay from high frequency to low frequency, we can calculate the phase velocity with which these structures are moving. When we applied cross-correlation analysis technique on iosodensity between Hyderabad and Allahabad, it suggested that there is an ~1 h delay between their correlations with reference to Allahabad station. Based on the distance between Allahabad and Hyderabad which is ~962 km and the time delay between their correlations, the horizontal propagation velocity works out to be on the order of 267 m/s, which is quite reasonable for TIDs. This suggests that given the magnitude of this storm, it is possible that TIDs could have propagated to low latitudes from high latitudes due to Joule heating.
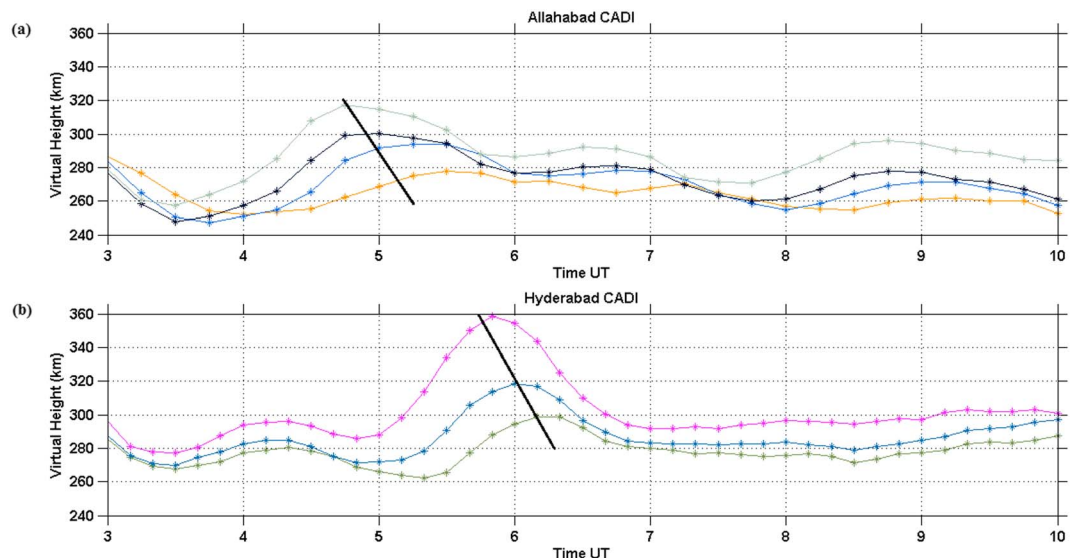

Figure 7. The temporal variation of isodensity plot at (a) Allahabad (5–8 MHz) and (b) Hyderabad (5–7 MHz) stations, respectively. The black line indicates variation of phase velocity.
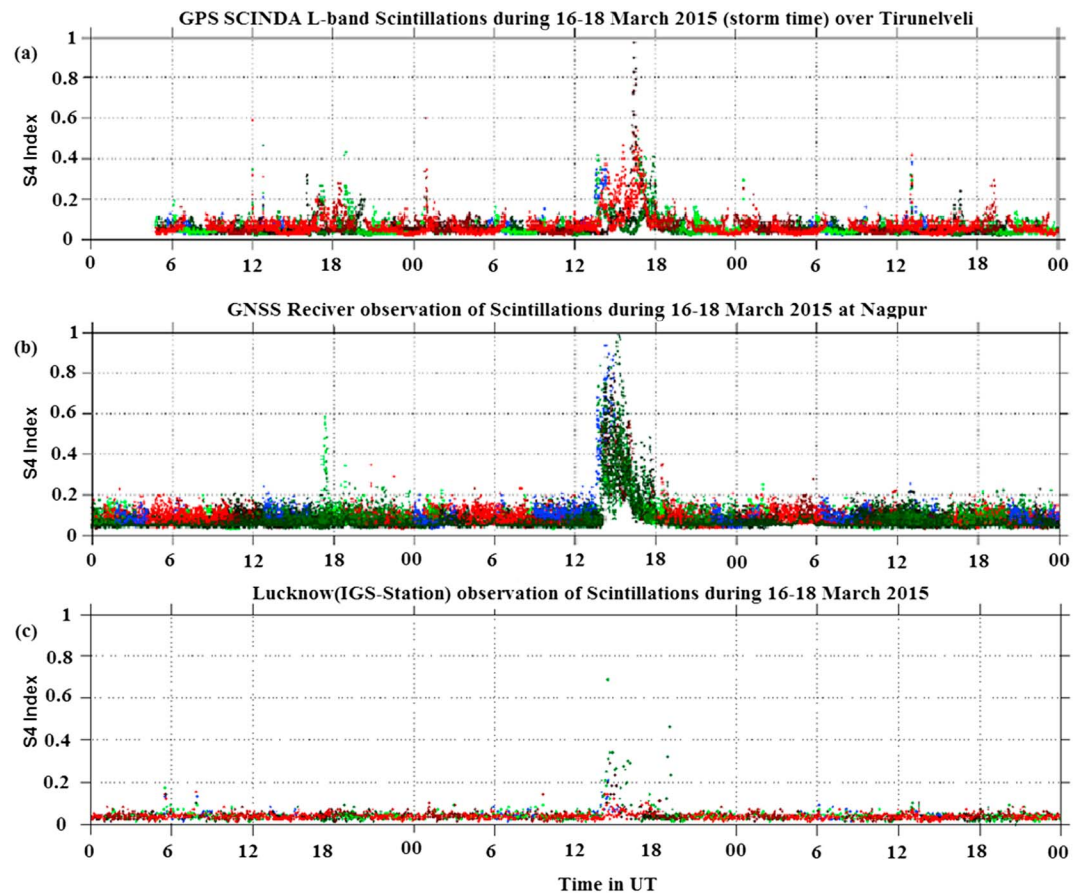
Figure 8. The GPS L band scintillations over (a) Tirunelveli, (b) Nagpur, and (c) Lucknow stations for the days 16–18 March 2015, respectively. Different colors indicate different PRNs.

3.3. Ionospheric Response as Seen by GPS Receivers
3.3.1. GPS L Band Scintillations

Figures 8a–8c show L band scintillations as represented by S_4 index over Tirunelveli, Nagpur, and Lucknow stations as obtained using GPS and GNSS receivers for the days 16–18 March 2015. The observations show weak scintillations on 16 March 2015 at Tirunelveli with S_4 index reaching to a value of 0.2–0.25 at 17:30–19:30 UT which is just above S_4 index threshold. But no L band scintillations are observed at Nagpur except for a patchy scintilations at 17:00 UT. However, on 17 March, scintillations started occurring at 14:00 UT and continued until 18:00 UT with S_4 index reaching near unity at 17:00 UT, suggesting severe scintillation behavior on this day. Very strong L band scintillations are recorded at the Nagpur station (which is ~2°E of Tirunelveli) just prior to the peak scintillations that occurred over Tirunelveli, indicating westward movement of the plasma irregularities which is in accordance with ionosonde zonal drifts as shown in Figure 4c. Interestingly, we do not see any scintillation at Lucknow except on 17 March, indicating the extent of scintillations. In the low-latitude zone, signal degradation may be more likely because of large variations in TEC near the crest of the EIA, owing to very large background densities. Correspondingly, scintillation index (S_4 index) also goes unity very easily.

3.3.2. GPS TEC Response

Figures 9a–9e show the temporal variation of GPS/GNSS vertical TEC from equator to beyond anomaly crest zone, namely, Tirunelveli (TIR), Bangalore (BAN), Hyderabad (HYD), Nagpur (NGP), and Lucknow (LKW), respectively, from top to bottom during 16–18 March 2015. Here it may be mentioned that we have applied elevation threshold of 30° so as to avoid multipath errors and the figure shows TEC above threshold. Different colors indicate different pseudo random noise (PRNs). There was a data gap on 16 March 2015 from 00:00 to 04:00 UT at Tirunelveli due to power failure, while TEC plots on 16 March show regular quiet time variations where TEC over TIR reduces during daytime due to fountain effect and
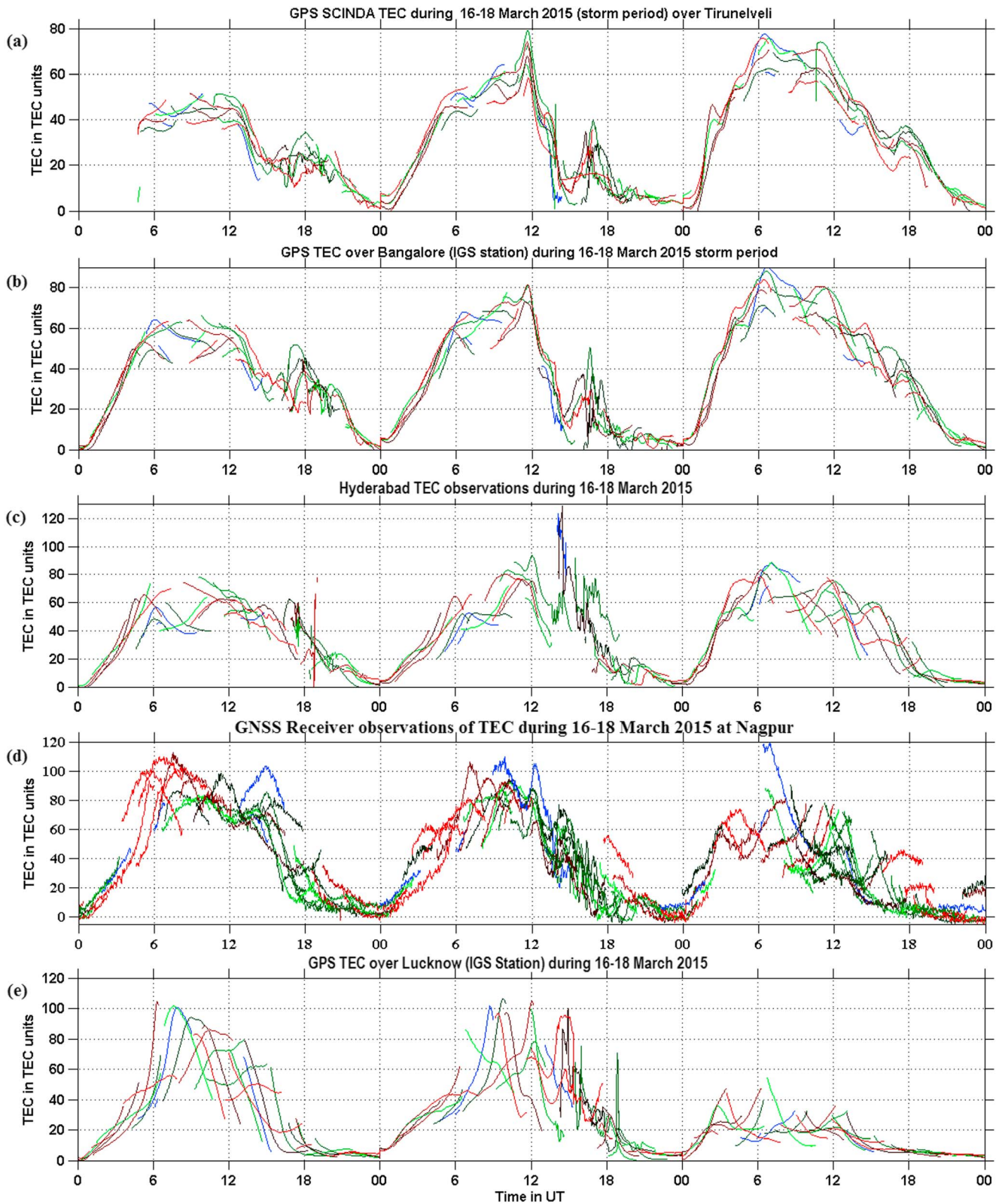
Figure 9. Temporal variations of GPS TEC over (a) Tirunelveli, (b) Bangalore, (c) Hyderabad, (d) Nagpur, and (e) Lucknow during 16–18 March 2015.
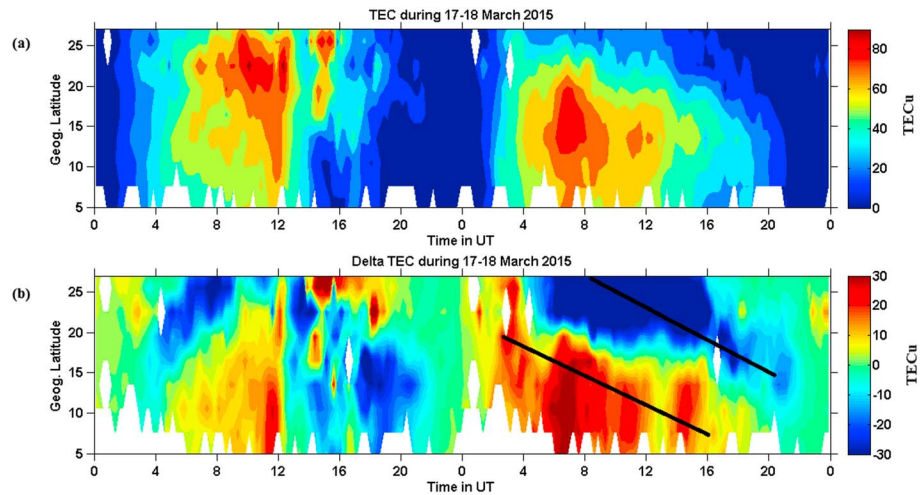
Figure 10. (a) The latitudinal and temporal variations of TEC (vertical) during 17–18 March 2015. (b) The delta TEC during 17–18 March 2015 after subtracting quiet day TEC (here it is 16 March). The black line indicates variation of phase velocity.

causes increase of TEC at other low-latitude stations like BAN/HYD/NGP/LKW. However, in the postsunset, large TEC fluctuations at TIR are seen due to strong scintillations as can be seen in the previous figure. However, story is different on 17 March. Initially, TEC varied quite normally. But after the SSC at 4:45 UT on 17 March, TEC showed sudden increase in its value at 06:00, 09:00, 12:00, and 14:00 UT at TIR which are also reflected in all other stations. This increase is abrupt at 12:00 UT than any other time. Since all the GPS receivers have shown these enhancements at nearly same time, these enhancements are believed to be caused by electric field-driven variation. This happens during the main phase. The observations show significant TEC enhancements of ~20 total electron content unit, $1\,\mathrm{TECU} = 10^{16}\,\mathrm{el\,m^{-2}}$ at almost all the stations at 12:00 UT during the storm day as compared to the other days. Over Tirunelveli, when the mean TEC values go up to nearby 50 TECU on quiet day (16 March), the storm day and the following day were characterized by 80 TECU. Similarly, over Bangalore, which is just outside equator and nearby Tirunelveli, TEC shows almost similar ranges of enhancements on the storm day and the next day. But at Hyderabad, it shows similar features as of Bangalore on 16 March but it showed decrease of TEC on 17 March as compared to Bangalore station. Nagpur TEC showed anomaly crest features where TEC increases of 100 TECU are seen on 16 and 17 March but reduction of TEC on 18 March. These features are almost seen at Lucknow except on 18 March, where TECs are drastically reduced as compared to Nagpur. It is believed that eastward electric field mapped due to the PP to low latitudes during daytime can push the ionization to higher altitudes through the upward $E \times B$ drift where recombination rates are low, causing additional plasma to be generated by solar illumination, resulting in a net increase of electron density (positive storm), consistent with our observations. On storm day, TEC enhancements were seen at Tirunelveli, Bangalore, Hyderabad, and Lucknow stations nearly 2 h earlier than the other 2 days. Since the strong PRE drives strong postsunset anomaly crests at low latitudes, these enhancements could be associated with PRE-related EIA enhancements. On the other hand, in general, Nagpur is characterized by ~100 TECU. On 18 March, TEC is not well pronounced as compared to storm day and it is varied at ~80 TECU. Recovery phase happens on 18 March, which is characterized by an increase in TEC at equatorial stations, namely, TIR and BAN, while a low latitude stations like NGP which lies in the anomaly crest zone and LKW which lies in the northern edge of the anomaly crest, a decrease in TEC values is shown. Overall, the TEC plots show the inverse relation between equatorial and low-latitude stations where TEC increase (decrease) at equator is related to TEC decrease (increase) at low latitudes.

Figures 10a and 10b show the latitudinal and temporal variations of mean (a) VTEC and (b) delta TEC map obtained on 17–18 March 2015 after taking chain of GPS stations as mentioned in the Table 1 over Indian region. The different colors represent whether TEC is enhanced (red color) or suppressed (blue color). It may be mentioned that the temporal resolution of 15 min, elevation angle of 30°, and longitude of 75–85°E are used while generating this map. We considered 16 March 2015 as our control or reference day and is subtracted from the TEC map to get delta TEC as shown in Figure 10b. From the

figure, it is evident that TEC shows well-developed EIA crests up to 23°N latitudes on 17 March 2015. But due to sudden enhancement in TEC at 12:00 UT, it is also seen as red patch at all the latitudes. In the evening hours, due to strong PRE drifts, TEC enhancements are seen at low latitudes between 16 and 25°N at 14:00–15:00 UT. The delta TEC map shows that there is a strong TEC enhancement at 12:00 UT related to storm. TEC enhancements in the postsunset hours indicate that they are indeed enhanced due to strong PRE. However, on 18 March 2015, the TEC is enhanced from 06:00 to 08:00 UT (11:30–14:30 LT) at latitudes below 20°N. After that, TEC got reduced drastically and latitudinal extent also got reduced unlike 17 March 2015. No postsunset enhancement is seen on 18 March 2015. The delta TEC also suggests that on 18 March, TECs are concentrated close to equatorial latitudes and strong reduction in TEC is seen at other latitudes. When we see the reduction of TEC from high latitudes to low latitudes, it shows clearly that TEC is reduced in an arranged manner. When we calculate the phase propagation from low latitude to equator using the slant line method (plotted in black line), it works out to be 1 h time which is quite similar to that of TIDs as seen in ionosondes.

4. Discussions

From the results as shown above, it is seen that changes in equatorial dynamics are evident during this storm where its effect has been observed right from the equator to the low latitudes. The results presented in the previous section indeed suggest that our results are unique in the sense that we have presented all the supporting evidence to show that there were strong PP electric fields that are penetrated to equator due to this geomagnetic storm during main phase and TID propagation to equatorward during recovery phase. Even when we examined the storm time IEFy electric fields, EEJ strength, and virtual height oscillations at single frequency (not shown here), it suggests that they are indeed varying as per IEFy oscillations during main phase. So these results suggest that we were encountering continuous penetration of electric fields on 17 March since 06:00 UT. In addition, the uniqueness of this storm is that it occurred at a time when PRE electric fields are usually intense over Indian sector and penetration efficiency of PP electric fields to equator is strong. Further, this storm occurred during equinox month where strong PRE electric fields are usually seen which produces intense plasma irregularities. Hence, delineating the storm time variations from quiet time is difficult due to strong coupling. However, this storm is so intense that we have seen elevated heights during PRE time which are quite different from regular ones and can be separated easily from other variations. From the observations presented above, it is seen that turning of IMF B_z from north to south drastically affects the low latitudes during both main and recovery phases. Since southward turning was sustained for quite long, it significantly affected low latitudes in terms of electric fields and winds. The important observations from the above analysis are (a) enhanced PRE drift of ~70 m/s at the postsunset hours and associated TEC enhancements at anomaly crests possibly associated with PP electric fields adding to the existing PRE electric fields, (b) F_3 layer occurrence during daytime associated with undershielding effect, (c) depression in magnetic data in association with overshielding, (d) occurrence of strong plasma bubbles or scintillations, (e) westward zonal drifts in the late night on 17 March, (f) gravity wave signatures in meridional winds, and (g) TID signatures at low latitudes during recovery phase.

In order to further understand these results, we examined storm time characteristics obtained for such major storms earlier at different longitudes. *Tsurutani et al.* [2004] suggested that PP electric field contributed to TEC increase and upliftment of the *F* layer. While studying the ionospheric response to the Halloween storm during October 2003, *Mannucci et al.* [2005] reported that the storm time PP could be a contributor of increased TEC at midlatitudes due to super fountain effect. But it has been also shown that PP electric fields during daytime from high to low latitudes as a contributing factor to TEC increase [*Fejer*, 2002; *Fejer and Scherliess*, 1997]. Our observations as presented in this paper also suggest similar enhancements in TEC briefly at 12:00–14:00 UT (IST: 17:30–19:30 h), indicating the role of PP electric fields in enhancing TEC during evening hours over Indian sector. But interestingly, our observations show that TEC does not increase to very high value, unlike that of *Tsurutani et al.* [2004]. This could be partly due to weak efficiency of PP electric fields during daytime unlike in the evening PP electric fields. *Raghavarao and Sivaraman* [1973] reported the development of strong EIA, which they attributed to the role of the PP electric field during main phase of the storm. Similarly, in our results, it is clear that EIA crest is shifted to approximately 23° latitudes. This result agrees better with the observations made by *Balan et al.* [2010], where they report that, if daytime eastward PP electric fields occur, it can result in the shifting of EIA crest to nearby 20° latitudes. Unlike American sector where usually strong TEC enhancements

of 200–300 TECU were observed, we did not notice such strong TEC enhancements during daytime in Indian sector during this storm. One of the possibilities could be the lower B field over Indian sector as compared to American sector. Other possibility could be as suggested by *Fejer et al.* [2007] that to have appreciable increase of TEC over equator, it depends on additional parameters such as magnetospheric and ionospheric conductivity variations. In addition, they suggested that PP electric fields will be significant during dusk-dawn hours due to enhanced conductivity gradients. They further suggested that although PP electric fields are driven by the solar wind and magnetospheric processes, their local time, duration, and strength are controlled by the polar cap potential which in turn depends on conductivity of the ring current which is proportional to the plasma sheet temperature and density and on ionospheric conductivity. So apart from convection electric fields, other ionospheric parameters such as conductivities are also vital for its impact on low latitudes. From our observations, it is seen that as soon as the IMF B_z turned southward (main phase), EEJ strength increased up to nearly 110 nT and later on drastically reduced and it became westward or CEJ. This impact is seen in the ionosondes. A similar kind of enhancement is noticed in the EIA development as the drivers for both EIA and EEJ are the same, i.e., the zonal electric field [*Balan and Iyer*, 1983; *Rastogi and Klobuchar*, 1990]. Occurrence of CEJ in the evening hours on 17 March (main phase) could be attributed to the development of westward electric fields possibly related to sudden northward turning of IMF B_z during this period (overshielding). Recently, it has been reported by *Tulasi Ram et al.* [2012] that it is possible to have westward/downward drift in the lower altitudes but eastward/upward drift during storm periods and F_3 layer can occur. However, we did not see F_3 layer generation during the CEJ period unlike theirs. But immediately after that, we noticed strong scintillations indicating that strong upward drifts are present as IMF B_z showed strong fluctuations. Reduction of AL index at the same time also indicates onset of substorm activity which could have caused PRE to enhance over Indian longitudes.

Severe ESF has been observed over TIR on the storm day, i.e., 17 March followed by increased PRE vertical drift on the order of nearly 70 m/s, although short-duration, spread F irregularities were present over HYD and ALD also. This shows that increased value of PRE has taken F layer to higher altitudes where RT instability caused spread F occurrence. The increased drifts and electric fields might have added to the polarization electric field which plays a role in the upward rise of plasma bubbles, and hence, these bubbles might have reached the higher latitudes. In addition, *Abdu et al.* [1998b] have studied DP 2 electric field fluctuations during a geomagnetic storm and suggested that dusk sector conductivity gradients might cause enhancement in the electric field during evening hours and reduction of electric field during daytime. Since we have seen large drift of 70 m/s in our case, we do believe that such conductivity gradients might exist during this storm period. Careful observations showed that the peak of S_4 index at TIR is seen only after peak of the S_4 index observed at NGP/LKW, signifying that irregularities are moved westward on storm day. Both TIR and NGP data reveal the presence of scintillations on storm day as compared to other days with the scintillations being severe in NGP than TIR. In addition to spread F signatures, additionally, the enhanced TEC values due to strong PRE might contribute to such intense scintillations over NGP. It is well known that PP electric field of eastward/westward polarity will lead to an enhanced/reduced PRE due to which it results in generation/suppression of ESF. In contrast, during a superstorm of 30 October 2003, it is observed that intense PP electric fields caused abnormally larger vertical drift of nearly more than 1000 m/s, which did not produce any ESF signatures [*Abdu et al.*, 2003; *Abdu*, 2012]. Their finding suggests that in a rapidly raising F layer, RT instability may not operate in the bottomside gradient region.

On 18 March, i.e., during recovery phase, EEJ strength showed its increasing strength in the morning, but as time progresses, it further reduced to form CEJ, which is evidently lesser in magnitude than the storm day's CEJ. This feature is prevailing in the recovery phase of the storm, where the effect of westward DD electric field is still going on, although its strength has been decaying, which could have reduced the EEJ strength and suppression of EIA. However, it is seen that initially, the EIA tried to develop in the morning due to daytime vertical drifts and strong EEJ currents; however, later on, the EIA formation is weakened (not well developed) and all the ionization is concentrated only over narrow latitudes near equator. This implies the action of westward disturbance dynamo electric field during recovery phase. The westward electric field suppresses the EIA crests, and hence, density over equatorial latitudes increases. *Su Basu et al.* [2009] reported that the collapse of EIA is due to the reversal of daytime upward vertical drifts. *Sastri* [1988] suggested that westward DD electric fields as the cause of daytime reduced EEJ strength, and they also reported the EIA inhibition associated with this, whereas *Abdu et al.* [1995] reported that local interaction between disturbance

zonal westward wind and evening eastward wind is resulting in decreased PRE electric field, which inhibits the EIA formation as seen in our observations.

Another point to be considered during recovery phase is the oscillations in h_pF_2, $h'F$, and density where the role of the disturbance winds modifying thermospheric circulation plays an important role. These oscillations are observed when multiple substorms were occurring in the auroral latitude indicating that these oscillations could be related to Joule heating at auroral latitudes and their atmospheric disturbances at low latitudes. Due to these disturbances, conductivity distribution in ionosphere might be different due to thermospheric circulation. It is established fact that storm time TEC enhancements/suppressions at equatorial and low latitudes are related to the changes in the electric fields or chemical composition [e.g., *Bagiya et al.*, 2011; *Burns et al.*, 1995; *Galav et al.*, 2011]. It is possible to delineate the electric field-driven variations with that of wind-driven variations using multistation data. If variations are associated with winds, it can be observed with a delay. It may be mentioned that due to particle precipitation and Joule heating at auroral latitudes during polar cap potential drop, winds blow from high latitude to midlatitudes, where they generate Pederson currents due to westward winds. This results in charge accumulation toward equator resulting in the generation of westward $E \times B$ drift and eastward current. This results in anti-Sq current system that opposes the normal quiet time behavior. *Abdu et al.* [2003] have studied the westward drifts during geomagnetic storms over Brazilian sector and suggested that nighttime zonal drifts could be flowing in the westward direction than eastward due to disturbance dynamo winds due to the Coriolis force. In another study, *Abdu et al.* [1998a] studied the vertical and zonal drifts during geomagnetic disturbances during postmidnights and suggested that they undergo periodic oscillations as indicated by AU/AL index (AL is a better indicator of substorm activity, since it represents and hence it has been widely used to represent the substorm activity). Such oscillatory behavior is noticed in our observations in vertical/zonal drifts during postmidnight of 17 March and early morning of 18 March. Also, such small-scale oscillations were present at HYD and ALD stations during recovery phase of the storm, i.e., on 18 March. The isodensity plot and their cross-correlation analysis suggest that there is a strong correlation between their variations but with a time lag of ~1 h between these oscillations from ALD to HYD stations, suggesting that it could be due to the TIDs propagating from high latitude to low latitudes due to the disturbance winds. *Lei et al.* [2008] have studied the ionospheric oscillations in terms of large-scale traveling ionospheric disturbances using both observations and simulations for the 2006 geomagnetic storm. Their observations suggest that it is possible to have strong TIDs during nighttime than daytime due to lower atmospheric drag. It is also possible that these observed disturbance meridional winds as seen in our case might have generated the DD electric field through Joule heating over high latitudes which is opposite to regular Sq current system. Drastic reduction in the density during recovery phase suggests that DD electric fields are westward during daytime over Indian sector which caused suppression of density due to strong recombination at lower altitudes. Also, during disturbance winds, molecular N_2 concentration increases at thermosphere due to upward motion at high latitudes that causes recombination and reduction of density at low latitudes. Several authors have investigated the O/N_2 ratio during geomagnetic storms and suggested that molecular N_2 concentration increases during recovery phase due to global wind circulation. When we examined O/N_2 ratio for this storm period, it indicates enhancement of molecular N_2 on 18 March at midlatitudes (not shown here). So these results grossly agree with well-explained features during major geomagnetic storms but still need to be more understood. While we presented here some initial results, several aspects of the storm still need to be understood which is being investigated including modeling.

5. Summary and Conclusions

We studied the equatorial and low-latitude ionosphere response to one of the major geomagnetic storms of the current solar cycle that occurred on 17 March 2015, where Dst reached its minimum of -228 nT due to double-halo CMEs using chain of ionosondes and GPS receivers over India. The main findings of the study are as follows: The observations show the EEJ fluctuations as per IEFy electric fields during storm main phase due to undershielding effect. However, there was a strong CEJ in the afternoon possibly associated with IMF B_z turning northward due to overshielding effect. However, EEJ showed prolonged CEJ features on the next day characterized by westward DD electric fields during recovery phase. F_3 layer occurrence at Tirunelveli during main phase of the storm possibly indicates the electric field fluctuations due to PP electric fields.

Increased F layer height of ~560 km and increased vertical plasma drift of 70 m/s in Tirunelveli ionosonde seen during local PRE times indicate that these are triggered mainly by eastward PP electric fields due to abrupt changes in the IMF B_z. Following large vertical drift over equator, scintillations/ESF started occurring right from equator to Nagpur/Allahabad/Lucknow stations which is unusual. Nighttime westward zonal drifts seen around 17:00 UT on 17 March instead of usual eastward drift indicate westward thermospheric circulation during this period. Following strong vertical drifts over equator, enhanced EIA is seen during postsunset period indicating the PRE-related fountain effect on 17 March 2015 during main phase. The suppression of EIA on the next day can be related to the westward disturbance dynamo electric field where oscillatory behavior in density, h_pF_2, and $h'F$ during recovery phase are observed. Further analyses of chain of ionosondes suggest that these oscillations are related to traveling ionospheric disturbances with period of ~1 h. The analyses of chain of TEC data also suggest that they are related to TIDs. Phase variations with time in the delta TEC on 18 March also suggest that there is a strong TID propagating to the equator. Thermospheric meridional winds as calculated using two ionosondes suggest equatorward wind surge with oscillatory features resembling atmospheric gravity waves with period of 2 h.

References

Abdu, M. (2012), Equatorial spread F/plasma bubble irregularities under storm time disturbance electric fields, *J. Atmos. Sol. Terr. Phys.*, *75*, 44–56, doi:10.1016/j.jastp.2011.04.024.

Abdu, M. A. (1997), Major phenomena of the equatorial ionosphere-thermosphere system under disturbed conditions, *J. Atmos. Sol. Terr. Phys.*, *59*, 1505–1519.

Abdu, M. A., I. S. Batista, G. O. Walker, J. H. A. Sobral, N. B. Trivedi, and E. R. de Paula (1995), Equatorial ionospheric electric fields during magnetospheric disturbances: Local time/longitude dependences from recent EITS campaigns, *J. Atmos. Terr. Phys.*, *57*, 1065–1083.

Abdu, M. A., P. T. Jayachan, J. MacDoug, J. F. Cecil, and J. H. A. Sobral (1998a), Equatorial F region zonal plasma irregularity drifts under magnetospheric disturbances, *Geophys. Res. Lett.*, *25*(22), 4137–4140.

Abdu, M. A., H. Sastri, H. Luhr, H. Tachihara, T. Kitamura, N. B. Trivedi, and J. H. A. Sobral (1998b), *DP* 2 electric field fluctuations in the dusk-time dip equatorial ionosphere, *Geophys. Res. Lett.*, *25*(9), 1511–1514.

Abdu, M. A., I. S. Batista, H. Takahashi, J. MacDougall, J. H. Sobral, A. F. Medeiros, and N. B. Trivedi (2003), Magnetospheric disturbance induced equatorial plasma bubble development and dynamics: A case study in Brazilian sector, *J. Geophys. Res.*, *108*(A12), 1449, doi:10.1029/2002JA009721.

Araki, T., J. H. Allen, and Y. Araki (1985), Extension of a polar ionospheric current to the nightside equator, *Planet. Space Sci.*, *33*(1), 11–16.

Bagiya, M. S., K. N. Iyer, H. P. Joshi, S. V. Thampi, T. Tsugawa, S. Ravindran, R. Sridharan, and B. M. Pathan (2011), Low-latitude ionospheric-thermospheric response to storm time electrodynamical coupling between high and low latitudes, *J. Geophys. Res.*, *116*, A01303, doi:10.1029/2010JA015845.

Balan, N., and K. N. Iyer (1983), Equatorial anomaly in ionospheric electron content and its relation to dynamo currents, *J. Geophys. Res.*, *88*(A12), 10,259–10,262.

Balan, N., S. V. Thampi, K. Lynn, Y. Otsuka, H. Alleyne, S. Watanabe, M. A. Abdu, and B. G. Fejer (2008), F_3 layer during penetration electric field, *J. Geophys. Res.*, *113*, A00A07, doi:10.1029/2008JA013206.

Balan, N., K. Shiokawa, Y. Otsuka, T. Kikuchi, D. Vijaya Lekshmi, S. Kawamura, M. Yamamoto, and G. J. Bailey (2010), A physical mechanism of positive ionospheric storms at low latitudes and midlatitudes, *J. Geophys. Res.*, *115*, A02304, doi:10.1029/2009JA014515.

Basu, S., et al. (2001), Ionospheric affects of major magnetic storms during the International Space Weather Period of September and October 1999: GPS observations, VHF/UHF scintillations, and in situ density structures at middle and equatorial latitudes, *J. Geophys. Res.*, *106*(A12), 30,389–30,413.

Basu, S., S. Basu, J. Huba, J. Krall, S. E. McDonald, J. J. Makela, E. S. Miller, S. Ray, and K. Groves (2009), Day-to-day variability of the equatorial ionization anomaly and scintillations at dusk observed by GUVI and modeling by SAMI3, *J. Geophys. Res.*, *114*, A04302, doi:10.1029/2008JA013899.

Batista, I. S., E. R. de Paula, M. A. Abdu, N. B. Trivedi, and M. E. Greenspan (1991), Ionospheric effects of the March 13, 1989, magnetic storm at low and equatorial latitudes, *J. Geophys. Res.*, *96*(A8), 13, 943–13,952.

Blanc, M., and A. D. Richmond (1980), The ionospheric disturbance dynamo, *J. Geophys. Res.*, *85*(A4), 1669–1686.

Buonsanto, M. J. (1999), Ionospheric storms—A review, *Space Sci. Rev.*, *88*, 563–601.

Burns, A. G., T. L. Killeen, W. Deng, G. R. Carignan, and R. G. Roble (1995), Geomagnetic storm effects in the low to middle latitude upper thermosphere, *J. Geophys. Res.*, *100*(A8), 14,673–14, 691.

Fejer, B. G. (2002), Low latitude storm time ionospheric electrodynamics, *J. Atmos. Sol. Terr. Phys.*, *64*, 1401–1408.

Fejer, B. G., and L. Scherliess (1997), Empirical models of storm time equatorial zonal electric fields, *J. Geophys. Res.*, *102*(A11), 24,047–24,056.

Fejer, B. G., M. F. Larsen, and D. T. Farley (1983), Equatorial disturbance dynamo electric fields, *Geophys. Res. Lett.*, *10*(7), 537–540.

Fejer, B. G., J. W. Jensen, T. Kikuchi, M. A. Abdu, and J. L. Chau (2007), Equatorial ionospheric electric fields during the November 2004 magnetic storm, *J. Geophys. Res.*, *112*, A10304, doi:10.1029/2007JA012376.

Fuller-Rowell, T. J., M. V. Codrescu, R. J. Moffett, and S. Quegan (1994), Response of the thermosphere and ionosphere to geomagnetic storms, *J. Geophys. Res.*, *99*(A3), 3893–3914.

Galav, P., S. Sharma, and R. Pandey (2011), Study of simultaneous penetration of electric fields and variation of total electron content in the day and night sectors during the geomagnetic storm of 23 May 2002, *J. Geophys. Res.*, *116*, A12324, doi:10.1029/2011JA017002.

Huang, C.-S. (2008), Continuous penetration of the interplanetary electric field to the equatorial ionosphere over eight hours during intense geomagnetic storms, *J. Geophys. Res.*, *113*, A11305, doi:10.1029/2008JA013588.

Huang, C.-S., J. C. Foster, and M. C. Kelley (2005), Long-duration penetration of the interplanetary electric field to the low-latitude ionosphere during the main phase of magnetic storms, *J. Geophys. Res.*, *110*, A11309, doi:10.1029/2005JA011202.

Huang, C.-S., J. C. Foster, and Y. Sahai (2007), Significant depletions of the ionospheric plasma density at middle latitudes: A possible signature of equatorial spread F bubbles near the plasmapause, *J. Geophys. Res.*, *112*, A05315, doi:10.1029/2007JA012307.

Kelly, M. C., B. G. Fejer, and C. A. Gonzalez (1979), An explanation for anomalous equatorial ionospheric electric fields associated with the northward turning of the interplanetary magnetic field, *Geophys. Res. Lett.*, *6*(4), 301–304.

Kikuchi, T. (1986), Evidence of transmission of polar electric fields to the low latitude at times of geomagnetic sudden commencements, *J. Geophys. Res.*, *91*(A3), 3101–3105.

Kikuchi, T., H. Luehr, T. Kitamura, O. Saka, and K. Schlegel (1996), Direct penetration of the polar electric field to the equator during a *DP* 2 event as detected by the auroral and equatorial magnetometer chains and the EISCAT radar, *J. Geophys. Res.*, *101*(A8), 17,161–17,173.

Kikuchi, T., K. H. Hashimoto, and K. Nazoki (2008), Penetration of magnetospheric electric fields to the equator during a geomagnetic storm, *J. Geophys. Res.*, *113*, A06214, doi:10.1029/2009JA014562.

Krishna Murthy, B. V., S. S. Hari, and V. V. Somayajulu (1990), Nighttime equatorial thermospheric meridional winds from ionospheric $h'F$ data, *J. Geophys. Res.*, *95*(A4), 4307–4310, doi:10.1029/JA095iA04p04307.

Lee, C. C., J. Y. Liu, B. W. Reinisch, Y. P. Lee, and L. B. Liu (2002), The propagation of traveling atmospheric disturbances observed during April 6–7, 2000 ionospheric storm in the West Pacific region, *Geophys. Res. Lett.*, *29*(5), 1068, doi:10.1029/2001GL013516.

Lei, J., A. G. Burns, T. Tsugawa, W. Wang, S. C. Solomon, and M. Wiltberger (2008), Observations and simulations of quasi periodic ionosphere oscillations and large-scale traveling ionospheric disturbances during the December 2006 geomagnetic storm, *J. Geophys. Res.*, *113*, A06310, doi:10.1029/2008JA013090.

Lin, C. H., A. D. Richmond, R. A. Heelis, G. J. Bailey, G. Lu, J. Y. Liu, H. C. Yeh, and S. Y. Su (2005), Theoretical study of the low- and midlatitude ionospheric electron density enhancement during the October 2003 storm: Relative importance of the neutral wind and the electric field, *J. Geophys. Res.*, *110*, A12312, doi:10.1029/2005JA011304.

Mannucci, A.J., B. T. Tsurutani, B. A. Iijima, A. Komjathy, A. Saito, W. D. Gonzalez, F. L. Guarnieri, J. U. Kozyra, and R. Skoug (2005), Dayside global ionospheric response to the major interplanetary events of October 29–30, 2003 "Halloween storms," *Geophys. Res. Lett.*, *32*, L12S02, doi:10.1029/2004GL021467.

Mikhailov, A. V., and K. Schlegel (1998), Physical mechanism of strong negative storm effects in the daytime ionospheric F_2 region observed with EISCAT, *Ann. Geophys.*, *16*, 602–608.

Raghavarao, R., and M. R. Sivaraman (1973), Enhancement of the equatorial anomaly in the topside ionosphere during magnetic storms, *J. Atmos. Terr. Phys.*, *86*, 2091–209.

Rastogi, R. G. (1974), Westward equatorial electrojet during daytime hours, *J. Geophys. Res.*, *79*(10), 1503–1512, doi:10.1029/JA079i010p01503.

Rastogi, R., and J. Klobuchar (1990), Ionospheric electron content within the equatorial F_2 layer anomaly belt, *J. Geophys. Res.*, *95*(19), 19,045–19,052.

Richmond, A. D., and S. Matsushita (1975), Thermospheric response to a magnetic substorm, *J. Geophys. Res.*, *80*(19), 2839–2850.

Rishbeth, H., R. A. Heelis, J. J. Makela, and S. Basu (2010), Storming the Bastille: The effect of electric fields on the ionospheric *F*-layer, *Ann. Geophys.*, *28*, 977–981.

Sastri, J. H. (1988), Equatorial electric-fields of ionospheric disturbance dynamo origin, *Ann. Geophys.*, *6*(6), 635–642.

Sastri, J. H., N. Jyoti, V. V. Somayajulu, H. Chandra, and C. V. Devasia (2000), Ionospheric storm of early November 1993 in the Indian equatorial region, *J. Geophys. Res.*, *105*(A8), 18,443–18,445, doi:10.1029/1999JA000372.

Sastri, J. H., K. Niranjan, and K. S. V. Subbarao (2002), Response of the equatorial ionosphere in the Indian (midnight) sector to the severe magnetic storm of July 15, 2000, *Geophys. Res. Lett.*, *29*(13), 1651, doi:10.1029/2002GL015133.

Somayajulu, V. V., C. A. Reddy, and K. S. Viswanathan (1987), Penetration of magnetospheric convective electric field to the equatorial ionosphere during the substorm of March 22, 1979, *Geophys. Res. Lett.*, *14*(8), 876–879.

Somayajulu, V. V., L. Cherian, K. Rajeev, G. Ramkumar, and C. Raghava Reddi (1993), Mean winds and tidal components during counter electrojet events, *Geophys. Res. Lett.*, *20*(14), 1443–1446.

Sreeja, V., C. V. Devasia, S. Ravindran, T. K. Pant, and R. Sridharan (2009), Response of the equatorial and low-latitude ionosphere in the Indian sector to the geomagnetic storms of January 2005, *J. Geophys. Res.*, *114*, A06314, doi:10.1029/2009JA014179.

Tsurutani, B., et al. (2004), Global dayside ionospheric uplift and enhancement associated with interplanetary electric fields, *J. Geophys. Res.*, *109*, A08302, doi:10.1029/2003JA010342.

Tsurutani, B. T., et al. (2006), Corotating solar wind streams and recurrent geomagnetic activity: A review, *J. Geophys. Res.*, *111*, A07S01, doi:10.1029/2005JA011273.

Tulasi Ram, S., N. Balan, B. Veenadhari, S. Gurubaran, S. Ravindran, T. Tsugawa, H. Liu, K. Niranjan, and T. Nagatsuma (2012), First observational evidence for opposite zonal electric fields in equatorial *E* and *F* region altitudes during a geomagnetic storm period, *J. Geophys. Res.*, *117*, A09318, doi:10.1029/2012JA018045.